

# No Evidence for Variability of Intervening Absorption Lines toward GRB 060206: Implications for the Mg II Incidence Problem \*

Kentaro AOKI,<sup>1</sup> Tomonori TOTANI,<sup>2</sup> Takashi HATTORI,<sup>1</sup> Kouji OHTA,<sup>2</sup>  
 Koji S. KAWABATA,<sup>3</sup> Naoto KOBAYASHI,<sup>4</sup> Masanori IYE,<sup>5</sup> Ken'ichi NOMOTO,<sup>6</sup>  
 and  
 Nobuyuki KAWAI<sup>7</sup>

<sup>1</sup>*Subaru Telescope, National Astronomical Observatory of Japan,  
 650 North A'ohoku Place, Hilo, HI 96720, U.S.A.*

<sup>2</sup>*Department of Astronomy, Kyoto University,  
 Sakyo-ku, Kyoto 606-8502*

<sup>3</sup>*Hiroshima Astrophysical Science Center, Hiroshima University,  
 1-31-1 Kagamiyama, Higashi-Hiroshima, Hiroshima 739-8526*

<sup>4</sup>*Institute of Astronomy, University of Tokyo,  
 2-21-1, Osawa, Mitaka, Tokyo*

<sup>5</sup>*National Astronomical Observatory of Japan,  
 2-21-1, Osawa, Mitaka, Tokyo*

<sup>6</sup>*Institute for the Physics and Mathematics of the Universe,  
 University of Tokyo, 5-1-5 Kashiwanoha, Kashiwa, Chiba 277-8568*

<sup>7</sup>*Department of Physics, Tokyo Institute of Technology,  
 2-12-1 Ookayama, Meguro-ku, Tokyo 152-8551*

(Received 2008 December 1; accepted )

## Abstract

We examine variability of absorption line strength of intervening systems along the line of sight to GRB 060206 at  $z = 4.05$ , by the low-resolution optical spectra obtained by the Subaru telescope from six to ten hours after the burst. Strong variabilities of Fe II and Mg II lines at  $z = 1.48$  during  $t = 5-8$  hours have been reported for this GRB (Hao et al. 2007), and this has been used to support the idea of clumpy Mg II cloudlets that was originally proposed to explain the anomalously high incidence of Mg II absorbers in GRB spectra compared with quasars. However, our spectra with higher signal-to-noise ratio do not show any evidence for variability in  $t = 6-10$  hours. There is a clear discrepancy between our data and Hao et al. data in the overlapping time interval. Furthermore, the line strengths in our data are in good agreement with

those observed at  $t \sim 2$  hours by Thöne et al. (2008). We also detected Fe II and Mg II absorption lines for a system at  $z = 2.26$ , and these lines do not show evidence for variability either. Therefore we conclude that there is no strong evidence for variability of intervening absorption lines toward GRB 060206, significantly weakening the support to the Mg II cloudlet hypothesis by the GRB 060206 data.

**Key words:** gamma rays: bursts – galaxies: ISM

## 1. Introduction

The gamma-ray burst (GRB) has opened up a new window to probe high redshift universe, now reaching comparable redshifts with the studies by galaxies and quasars, and starting to probe the era of the cosmic reionization (Kawai et al. 2006). The optical GRB afterglow spectra give us a lot of information about GRB host galaxies (Mirabal et al. 2002; Savaglio, Fall, and Fiore 2003; Prochaska et al. 2007; Chen et al. 2007), intervening absorption systems along the line of sight (Prochter et al. 2006; Sudilovsky et al. 2007; Tejos et al. 2007) and the reionization of the universe (Totani et al. 2006).

GRB 060206 is the 10th highest redshift GRB as of 2008 November. GRB 060206 was triggered by the *Swift* Burst Alert Telescope on 2006 February 6 at 04:46:53 UT. The redshift of the burst was determined to be 4.048 (Fynbo et al. 2006). The intervening absorption lines are reported at  $z = 1.48$  (Fynbo et al. 2006; Hao et al. 2007; Thöne et al. 2008) and  $z = 2.26$  (Aoki et al. 2006; this work). Surprisingly, Hao et al. (2007) claimed strong variation of the equivalent widths (EWs) of Fe II  $\lambda 2600.2$  and Mg II  $\lambda 2803.5$  at  $z = 1.48$ ; the EW of the Fe II  $\lambda 2600.2$  system at  $z = 1.48$  showed a more than 80% decrease within 1.5 hours duration. It is difficult to interpret this system to be located in the GRB host galaxy, because a large redshift difference requires relativistic motion and hence a large velocity dispersion of lines is expected, while the absorption line widths are only  $14 - 20 \text{ km s}^{-1}$  (Thöne et al. 2008). Then, almost unique possible interpretation is that the intervening absorption system is smaller than the image size of the GRB afterglow, and the line strength changes with the size evolution of the GRB afterglow. This requires the size of the absorption system to be less than  $\sim 10^{16} \text{ cm}$  (Hao et al. 2007).

This variability, if real, would change the standard picture of intervening absorption systems found in bright cosmological objects such as quasars and GRBs. Furthermore, this result has been used to support the Mg II cloudlet hypothesis that has been proposed to explain the anomalous Mg II incidence along the GRB sight lines (Frank et al. 2007). Prochter et al. (2006) reported that the incidence of Mg II absorption lines along GRB sight lines is about four

---

\* Based on data collected at Subaru Telescope, which is operated by the National Astronomical Observatory of Japan.

times higher than that for quasars, at a statistical significance greater than 99.9% confidence limit, and this cannot easily be explained by known selection effects. If the intervening line variability of GRB 060206 is in fact due to the small size of the Mg II cloudlets, the anomalous incidence of Mg II systems may also be explained by the larger image size of quasars than GRB afterglows.

However, GRB 060206 is currently the only one case for the intervening line variability, and it should be examined carefully. Here we report the analysis of the optical afterglow spectra of GRB 060206 taken by the Subaru telescope during  $t = 6.01\text{--}9.73$  hours after the burst, a part of which is overlapping with the Hao et al.'s observation ( $t = 4.13\text{--}7.63$  hours). We will examine especially the line variability of the intervening Mg II and Fe II systems. In addition to the  $z = 1.48$  system, we will give detailed analysis of the  $z = 2.26$  system as well and examine the variability.

When we completed most of this paper, the revised version of Thöne et al. (2008, arXiv:0708.3448v2) appeared on the preprint server, in which they also analyzed the same data from the Subaru archive and reached a similar conclusion of no evidence for variability. However, details of the Subaru observation and data analysis are not given in their paper. Here we give more detailed descriptions about the observation logs and the processing of the Subaru data taken by ourselves, as well as the implications for the Mg II incidence problem. The  $z = 2.26$  system was originally reported by Aoki et al. (2006) and it is mentioned also in Fynbo et al. (2006), but Thöne et al. (2008) concluded that this is not real. However, we will show that this system is real, based on the detection of seven Fe II lines and Mg II doublet.

## 2. Observations and Data Reduction

The afterglow of GRB 060206 was observed on 2006 February 6 (UT) with FOCAS (Kashikawa et al. 2004) attached to the Subaru 8.2-m telescope (Iye et al. 2004). We obtained eight spectra of 30 minutes integration for each at 10:47, 11:19, 11:51, 12:23, 12:54, 13:28, 13:59, and 14:31 (UT). All these times are midpoint of exposures. We used the R300 grism with two different order-cut filters for the observations. The first three and last two spectra were taken with the O58 filter which covers between 5700 Å and 10200 Å. The other three spectra were taken with the Y47 filter which allows an uncontaminated spectrum between 4800 Å and 9200 Å. The slit width was set to be 0"8. The atmospheric dispersion corrector was used and the slit position angle was 176°. The spectrophotometric standard star Hz 44 was observed for sensitivity calibration and removal of atmospheric absorption lines. It was photometric condition with good seeing (0"6 - 0"9 in  $R$ -band). The seeing size became smaller as the GRB was rising, and it was smaller than the slit width at the final epoch of the observations. Consequently, the resolution of the GRB's spectra was changed from 8.0 Å to 6.8 Å (290 km s<sup>-1</sup> to 250 km s<sup>-1</sup> at 8190 Å), which is confirmed by measuring absorption lines of a bright star found in the same slit for the GRB afterglow.

The data were reduced using IRAF<sup>1</sup> for the procedures of bias subtraction, flat-fielding, wavelength calibration, and sky subtraction. Wavelength calibration was performed using OH night sky emission lines, and the rms wavelength calibration error is 0.2 - 0.3 Å. The sensitivity calibration was performed as a function of wavelength, and the atmospheric absorption feature was removed by using the spectrum of Hz 44. Fringe pattern exists beyond 7700 Å in the spectra, and fringe spectra were made from the standard star’s spectra normalized by its continuum. We divided the afterglow spectra by the fringe spectra, and suppressed the fringe pattern. The initial strength of fringe pattern is 6–11% of the continuum level of the afterglow spectra, but it is reduced by a factor of  $\sim 2$  by this process. The foreground Galactic extinction of  $A_B = 0.054$  mag (Schlegel, Finkbeiner, and Davis 1998) was corrected.

### 3. Results

Figure 1 displays the optical spectrum of GRB 060206 taken 9.7 hours after the burst. The absorption feature between 9300 and 9600 Å is residuals of the telluric absorption removal. The spectrum clearly shows the  $z = 4.05$  and  $1.48$  absorption line systems which have been reported by Fynbo et al. (2006), Hao et al. (2007), and Thöne et al. (2008). Furthermore, the  $z = 2.26$  absorption line system of Mg II is clearly recognized. We also detected seven Fe II resonance lines ( $\lambda\lambda 2249.9, 2260.8, 2344.3, 2374.5, 2382.8, 2586.7,$  and  $2600.2$ ) at  $z = 2.26$ . All these  $z = 2.26$  absorption lines are beyond 7200 Å and hence outside of the coverage of the WHT/ISIS observation (Fynbo et al. 2006; Thöne et al. 2008), explaining that Thöne et al. (2008) could not find the absorption system at  $z = 2.26$ . We list all detected lines in table 3 in Appendix. In figure 11 in Appendix, we show the spectrum combined all 4 hours data.

We show Fe II  $\lambda\lambda 2586.7, 2600.2$  absorption line profiles at  $z = 1.48$  in our normalized spectra in Figure 2. No significant temporal variation is seen between 6.0 and 9.7 hours after the burst. The absorption lines at 9.73 hours after the burst are narrower than those at other epochs, but this is due to the change of the spectral resolution; note that seeing size is smaller than the slit width at this epoch, as mentioned in Section 2. We also show Mg II  $\lambda\lambda 2796.4, 2803.5$  absorption lines at  $z = 1.48$  in Figure 3. No significant temporal variation is seen, either. We measured EW in the observer’s frame for these lines by fitting each absorption line with a single Gaussian. The Gaussian fits are shown in Figure 2 and 3, and the EW results are tabulated in table 1. Figure 4 presents the time evolution of EW of these lines, and we confirm that there is no significant variation in the strength of all the four  $z = 1.48$  absorption lines. The difference between the first and last observations is 0.14 Å at maximum (Mg II  $\lambda\lambda 2796.4$ ), and that is smaller than  $1\sigma$  uncertainty. The EW measurements of Mg II  $\lambda 2803.5$ , Fe II  $\lambda 2600.2$ , and Fe II  $\lambda 2586.7$  in the same Subaru data performed by Thöne et al. (2008) are mostly consistent with

---

<sup>1</sup> IRAF is distributed by the National Optical Astronomy Observatory, which is operated by the Association of Universities for Research in Astronomy (AURA), Inc., under cooperative agreement with the National Science Foundation.

our measurements. However, we find that the EW of Mg II  $\lambda 2796.4$  in Thöne et al. (2008) is significantly smaller than our measurement. The reason for this discrepancy is not clear, although the conclusions of no evidence for variability are the same.

The absorption line profiles of Fe II  $\lambda\lambda 2586.7, 2600.2$ , Mg II  $\lambda\lambda 2796.4, 2803.5$ , Fe II  $\lambda\lambda 2249.9, 2260.8$ , Fe II  $\lambda 2344.2$ , and Fe II  $\lambda\lambda 2374.5, 2382.8$ , for another intervening absorption line system at  $z = 2.26$  are shown in Figure 5, 6, 7, 8 and 9, respectively. The absorption line at  $8439 \text{ \AA}$  is Al II at  $z = 4.05$ , and those at  $7710 \text{ \AA}$  and  $7748 \text{ \AA}$  are Si II  $\lambda 1526.7$  and Si II\*  $\lambda 1533.4$  at  $z = 4.05$ , respectively. The equivalent widths are measured in the same way as the system at  $z = 1.48$ , and the results are listed in table 2. We do not find any systematic change of equivalent width in these all absorption lines at  $z = 2.26$  but one, either (Figure 10). The EW of Fe II  $\lambda 2382.8$  changed more than  $3\sigma$  between 6.0542 hours and 7.065 hours. Since the oscillator strength of Fe II  $\lambda 2374.5$  ( $3.13 \times 10^{-2}$ ) is smaller than that of Fe II  $\lambda 2382.8$  ( $3.20 \times 10^{-1}$ ), Fe II  $\lambda 2374.5$  is less saturated, and thus should be more variable than Fe II  $\lambda 2382.8$ . However, the EW of Fe II  $\lambda 2374.5$  was stable within  $1\sigma$ . As seen in Figure 9, Fe II  $\lambda 2382.8$  was heavily blended with Si II\*  $\lambda 1533.4$  at  $z = 4.05$ . This may cause larger uncertainty in EW, and large variation in Fe II  $\lambda 2382.8$  is doubtful. Note that Mg II  $\lambda 2803.5$  is systematically stronger than Mg II  $\lambda 2796.4$  in Figure 7, although the strength of Mg II  $\lambda 2803.5$  should be the same (optically thick case) as, or weaker (optically thin case) than, Mg II  $\lambda 2796.4$ . We noticed Si II  $\lambda 1808.01$  at  $z = 4.05$  is probably overlapped with Mg II  $\lambda 2803.5$  at  $9130.5 \text{ \AA}$ . Using the column density of Si II ( $1.7 \times 10^{15}$ ) from Thöne et al. (2008), we estimated EW of Si II  $\lambda 1808.01$  to be  $0.56 \text{ \AA}$  in observers' frame (optically thin case). We confirm that Si II  $\lambda 1808.01$  absorption line will be optically thin with the column density, the Doppler parameter  $b$  of  $20 \text{ kms}^{-1}$  and the small oscillator strength ( $2.08 \times 10^{-3}$ ). We consider that the contamination of Si II  $\lambda 1808.01$  is likely the cause of a systematic increase of Mg II  $\lambda 2803.5$  in this result.

#### 4. Discussion and Conclusion

In addition to the Subaru data, the equivalent width measurements of the  $z = 1.48$  system by Hao et al. (2007) and the WHT/ISIS data of Thöne et al. (2008) are shown in Figure 4. Our early four spectra are overlapping in time with the last three observations by Hao et al. (2007). Our EW measurement of  $z = 1.48$  Fe II  $\lambda 2600.2$  at  $t = 6.011$  hours is clearly in disagreement with the value measured by Hao et al. (2007) at  $t = 6.15$  hours. It should be noted that Fe II  $\lambda 2586.7$  at  $z = 1.48$  is clearly detected at  $6415 \text{ \AA}$  in our spectra (Figure 2) with an equivalent width of  $\sim 0.55 \text{ \AA}$ . On the other hand, it is not mentioned by Hao et al. (2007), and in fact, this line cannot be clearly seen in the Hao et al.'s spectra. This indicates that an EW of  $\lesssim 0.5 \text{ \AA}$  cannot reliably be measured by the Hao et al.'s observation, and hence the claim of the variability of Fe II  $\lambda 2600.2$  line should suffer from a large uncertainty.

The Hao et al.'s spectra show a strong variability of Mg II lines around  $t = 5 - 5.5$  hours, and we cannot examine this variability because this epoch is not covered by our data. However,

the early measurements of EWs of these lines at  $z = 1.48$  by Thöne et al. (2008) at  $t \sim 2$  hours are in good agreement with our measurements. It seems rather unlikely that the lines show a variability only in the time duration of the Hao et al.’s observation and no variability at all in the earlier or later data with higher signal-to-noise ratio. Furthermore, there is no evidence for time evolution of EWs in another absorption system at  $z = 2.26$ . From these results, we conclude that the variability reported by Hao et al. (2007) is likely due to some artificial effects or statistical fluke in low signal-to-noise data.

Our result implies that the data of GRB 060206 no longer provide a strong support to the MgII cloudlet hypothesis proposed by Frank et al. (2007) for the anomalously high incidence of MgII systems in GRB spectra. Furthermore, several difficulties of this hypothesis have been pointed out. One such argument is that apparently unsaturated MgII absorption lines with the doublet ratio of 1:1 are never found in intervening absorption lines, although such lines are expected if optically thick MgII cloudlets partially cover quasar beams (Prochter et al. 2006; Porciani, Viel, and Lilly 2007; Sudilovsky et al. 2007). Another argument is that there is no apparent change in MgII incidence over the continuum and broad emission lines of quasar spectra, although the broad line regions of quasars are much larger than the continuum emitting region (Pontzen et al. 2007). It should also be noted that the suggested size of the MgII cloudlets is several orders of magnitude smaller than those derived from the observations of gravitationally lensed quasars (Rauch et al. 2002; Ellison et al. 2004).

Therefore, we consider that the MgII incidence anomaly is likely to be explained by some other effects. Although the anomaly has not yet been solved, it could be explained, or at least the statistical significance of the anomaly is reduced, by a combination of some selection effects such as dust extinction and gravitational lensing (Porciani, Viel, and Lilly 2007; Sudilovsky et al. 2007).

We are grateful to the Subaru Telescope staff for their assistance during our observations. This work was partly supported by the Grant-in-Aid for Scientific Research on Priority Areas (19047003) from the Ministry of Education, Culture, Sports, Science and Technology (MEXT) of Japan.

## **Appendix. Absorption Lines List**

We identified absorption lines in the spectrum combined all 4 hrs data (Figure 11), but 1.5 hrs integration between 4800 Å and 6000 Å, and 2.5 hrs between 8800 Å and 10200 Å. The identifications, observed wavelengths in vacuum, and equivalent widths in rest frame are listed in Table 3. Most absorption lines redward of 7000 Å in GRB 060206 are reported here at the first time



## References

- Aoki, K., Hattori, T., Kawabata, K. S., & Kawai, N. 2006, GCN Circular, 4703
- Chen, H.-W., Prochaska, J. X., Ramirez-Ruiz, E., Bloom, J. S., Dessauges-Zavadsky, M., & Foley, R. 2007, ApJ, 663, 420
- Ellison, S. L., Ibata, R., Pettini, M., Lewis, G. F., Aracil, B., Petitjean, P. & Srianand, R. 2004, A&A, 414, 79
- Frank, S., Bentz, M. C., Stanek, K. Z., Mathur, S., Dietrich, M., Peterson, B. M., & Atlee, D. W. 2007, Ap&SS, 312, 325
- Fynbo, J. P. U., et al. 2006, A&A, 451, L47
- Hao, H., et al. 2007, ApJ, 659, L99
- Iye, M., et al. 2004, PASJ, 56, 381
- Kashikawa, N., et al. 2002, PASJ, 54, 819
- Kawai, N. et al. 2006, Nature, 440, 184
- Mirabal, N. et al. 2002, ApJ, 578, 818
- Pontzen, A., Hewett, P., Carswell, R., & Wild, V. 2007, MNRAS, 381, L99
- Porciani, C., Viel, M., and Lilly, S. J. 2007, ApJ, 659, 218
- Prochaska, J. X., Chen, H-W, Dessauges-Zavadsky, M., & Bloom, J. S. 2007, ApJ, 666, 267
- Prochter, G. E. et al. 2006, ApJL, 648, L93
- Rauch, M., Sargent, W. L. W., Barlow, T. A., & Simcoe, R. A. 2002, ApJ, 576, 45
- Savaglio, S., Fall, S. M., & Fiore, F. 2003, ApJ, 585, 638
- Schlegel, D. J., Finkbeiner, D. P., & Davis, M. 1998, ApJ, 500, 525
- Sudilovsky, V., Savaglio, S., Vreeswijk, P., Ledoux, C., Smette, A., & Greiner, J. 2007, ApJ, 669, 741
- Tejos, N., Lopez, S., Prochaska, J. X., Chen, H.-W., & Dessauges-Zavadsky, M. 2007, ApJ, 671, 622
- Thöne, C. C., et al. 2008, A&A, 489, 37
- Totani, T., Kawai, N., Kosugi, G., Aoki, K., Yamada, T., Iye, M., Ohta, K., & Hattori, T. PASJ, 58, 485

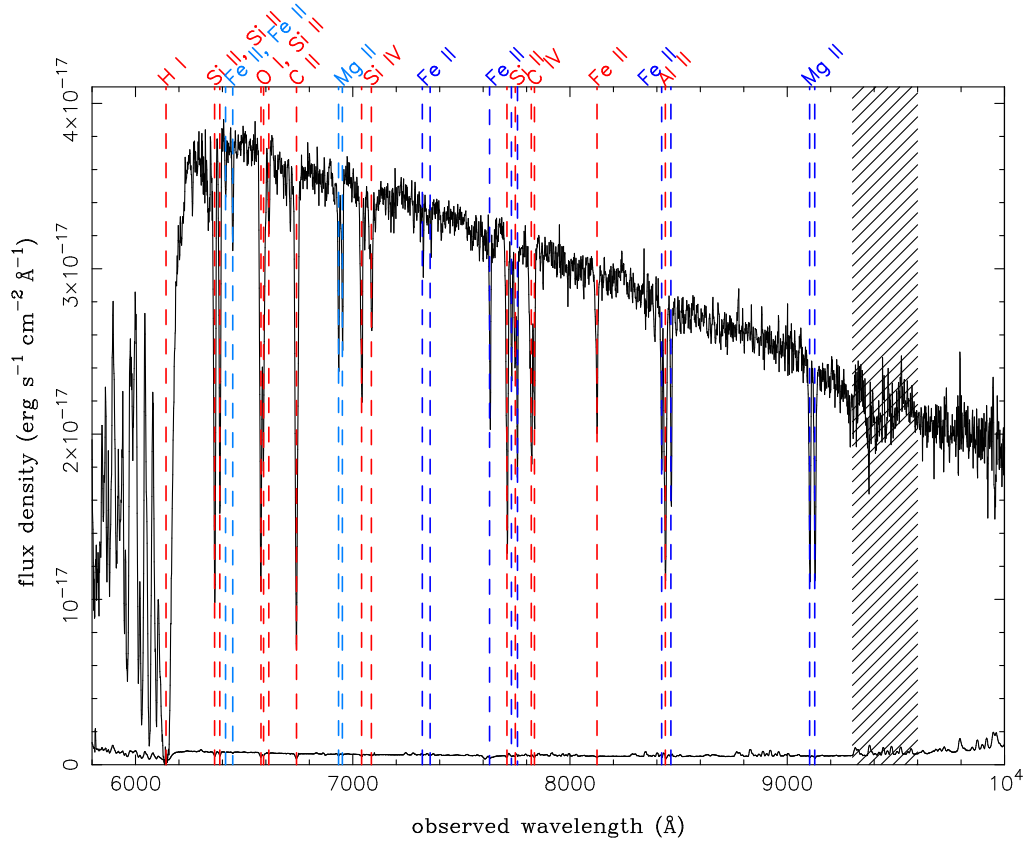


**Fig. 1.** The observed spectrum of GRB 060206 afterglow in vacuum wavelength. This spectrum was taken at 9.7 hours after the burst. Red, cyan, and blue dashed lines indicate absorption lines at  $z = 4.05, 1.48$  and  $2.26$ , respectively. The hatched region between  $9300$  and  $9600$  Å indicates the place of water vapor absorption lines in the atmosphere. The spectrum at the bottom is the noise spectrum.



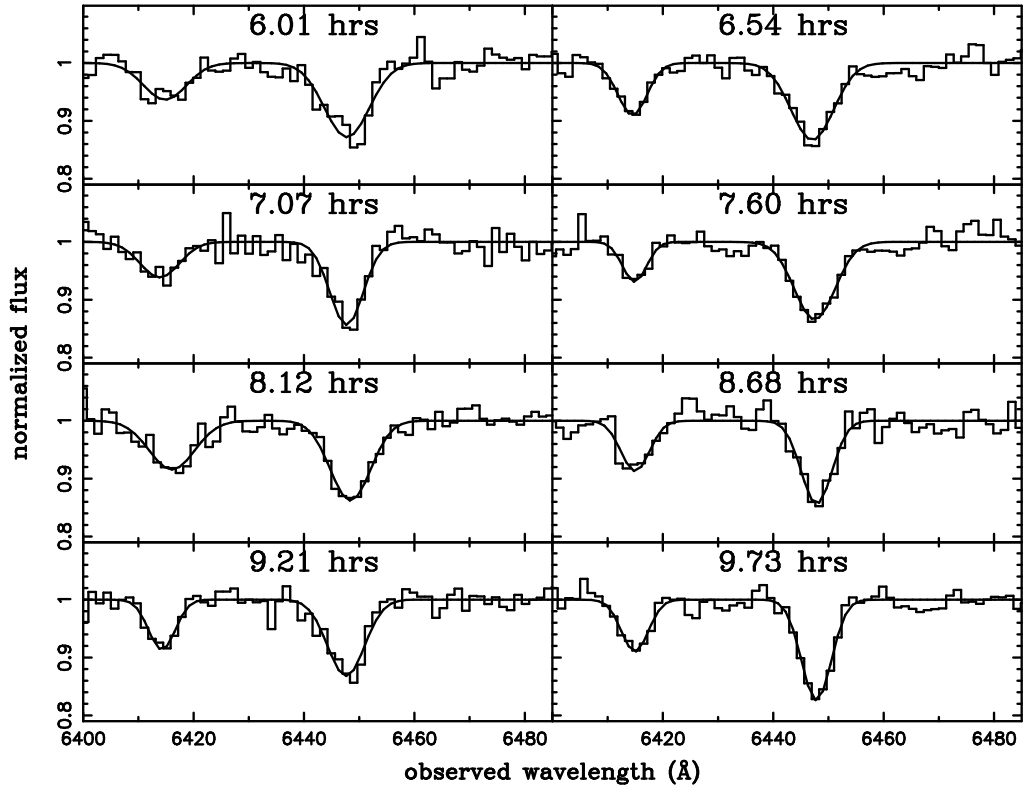


**Fig. 2.** Spectra of GRB 060206 afterglow around FeII  $\lambda\lambda 2586.7, 2600.2$  at  $z = 1.48$ . All spectra are normalized by the continuum, and all absorption lines are fitted with a Gaussian.

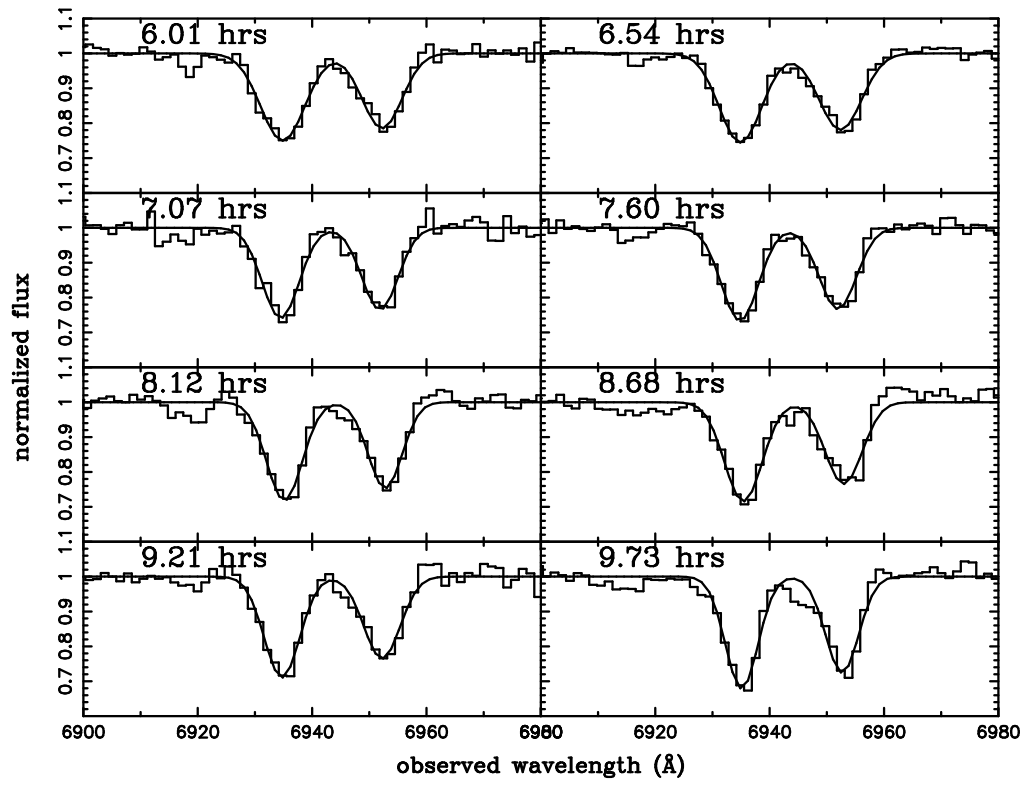
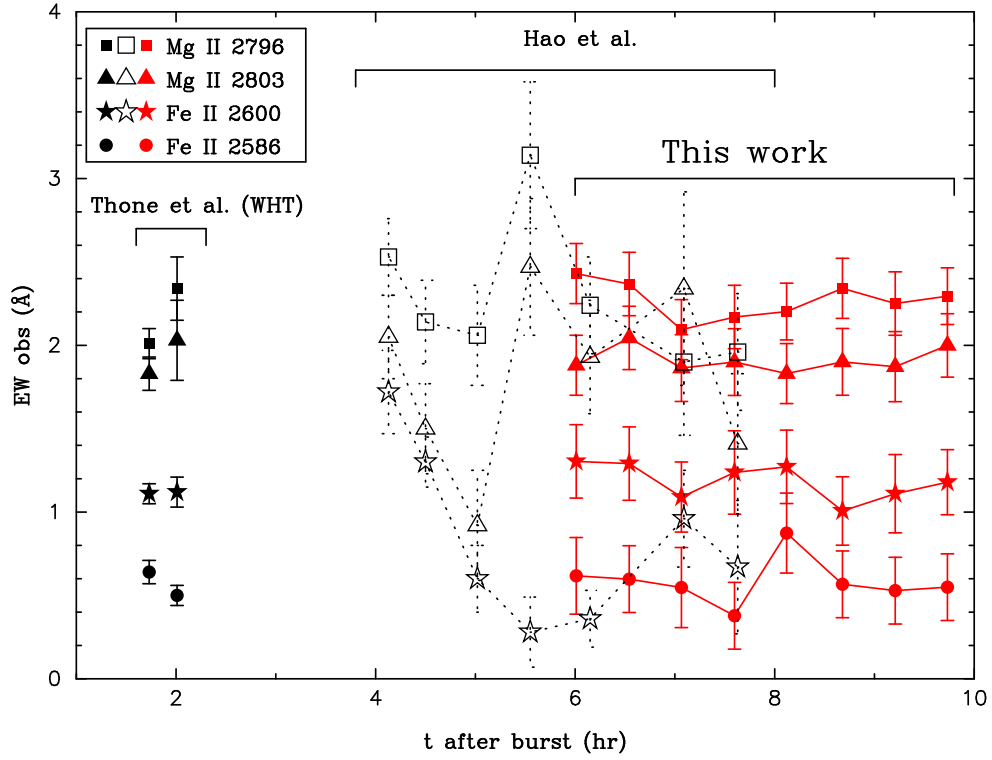


Fig. 3. The same as Fig. 2, but for Mg II  $\lambda\lambda 2796.4, 2803.5$  at  $z = 1.48$ .



**Fig. 4.** Equivalent width (observer’s frame) of the  $z = 1.48$  absorption lines versus observation time after the burst. The EWs of Fe II  $\lambda\lambda 2586.7, 2600.2$ , and Mg II  $\lambda\lambda 2796.4, 2803.5$  are shown with the symbols indicated in the figure. Our measurements are indicated by filled red symbols between 6 hours and 10 hours, and Hao et al. (2007) data by open ones between 4 hours and 8 hours. The filled black symbols at 2 hours are from Thöne et al. (2008).

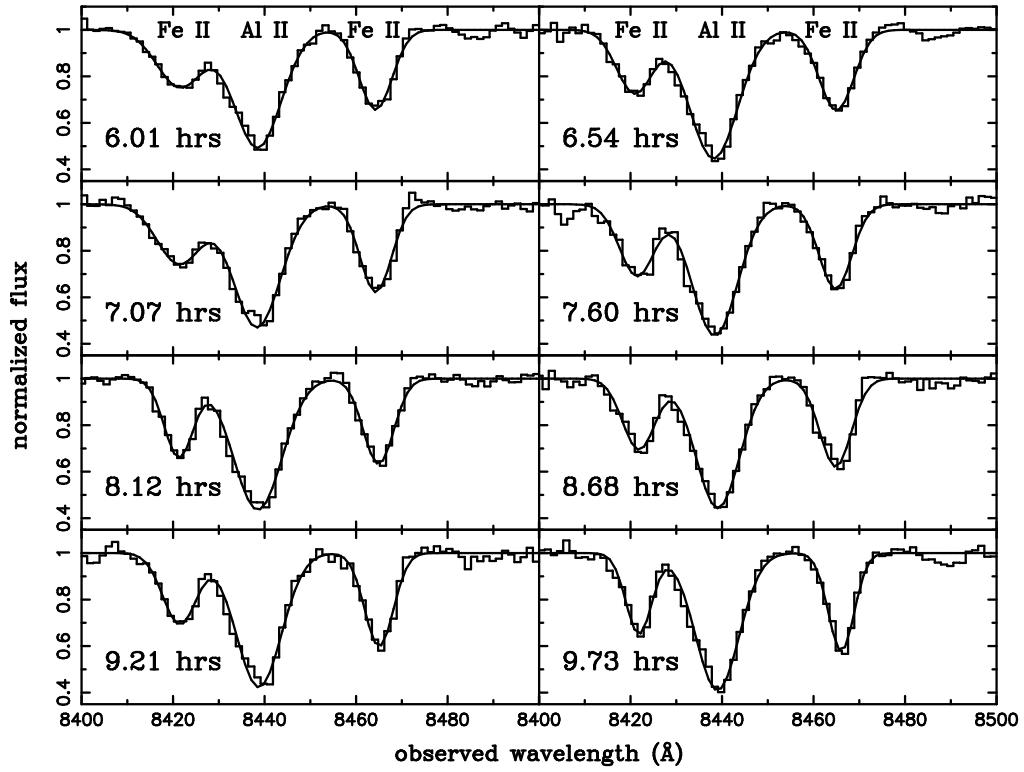


Fig. 5. The same as Fig. 2, but for Fe II  $\lambda\lambda 2586.7, 2600.2$  at  $z = 2.26$ . The absorption line at  $8439 \text{ \AA}$  is Al II at  $z = 4.05$ .

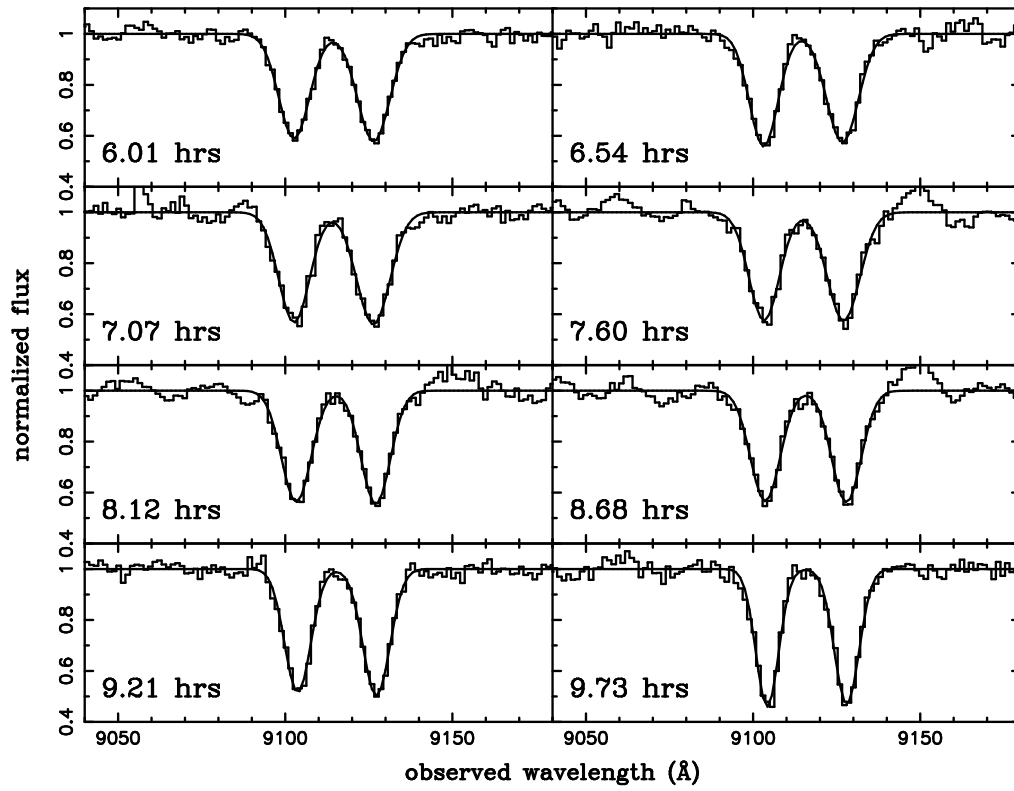


Fig. 6. The same as Fig. 2, but for Mg II  $\lambda\lambda 2796.4, 2803.5$  at  $z = 2.26$ .

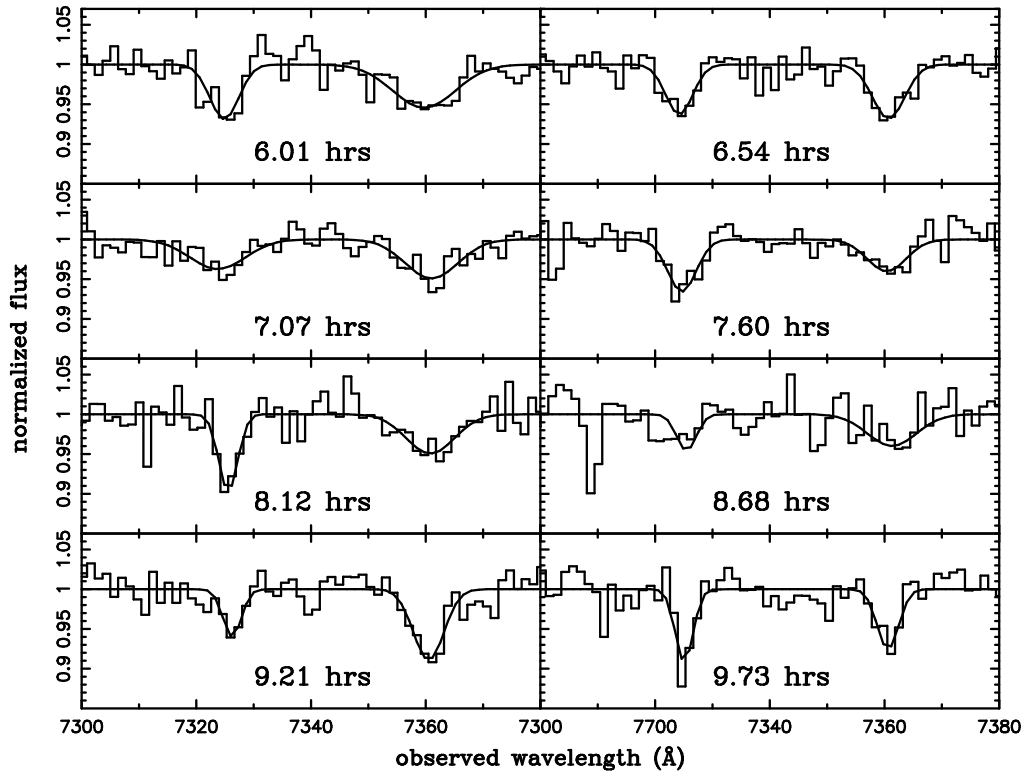


Fig. 7. The same as Fig. 2, but for Fe II  $\lambda\lambda 2249.9, 2260.8$  at  $z = 2.26$ .

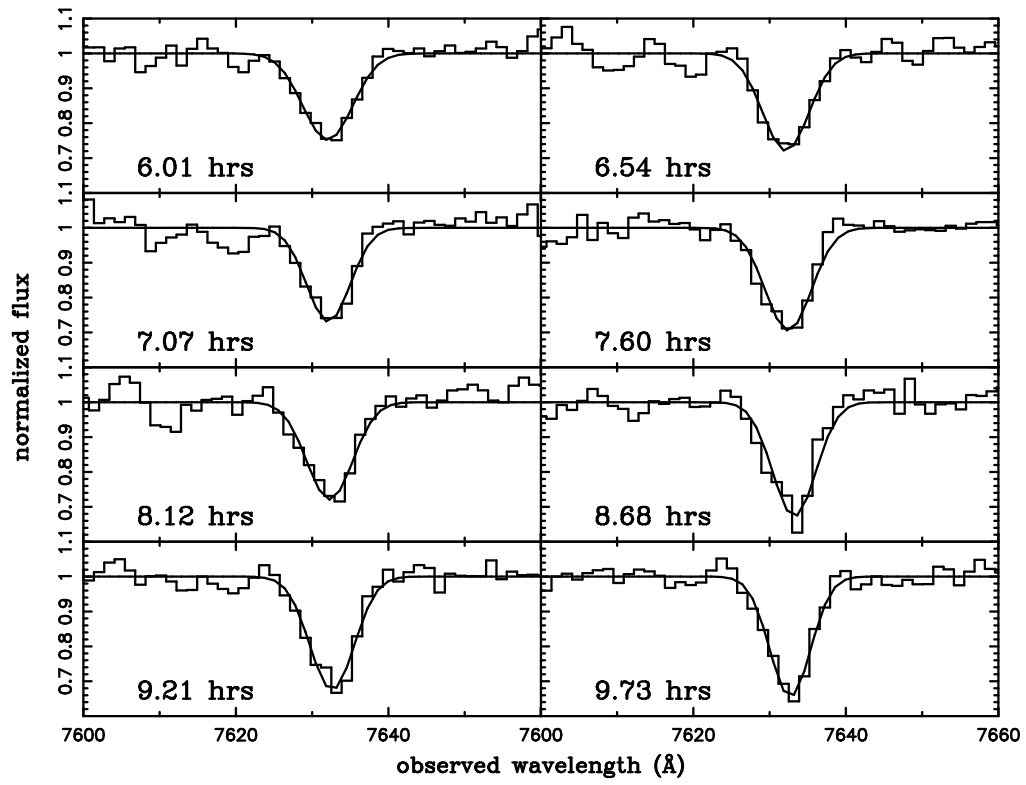
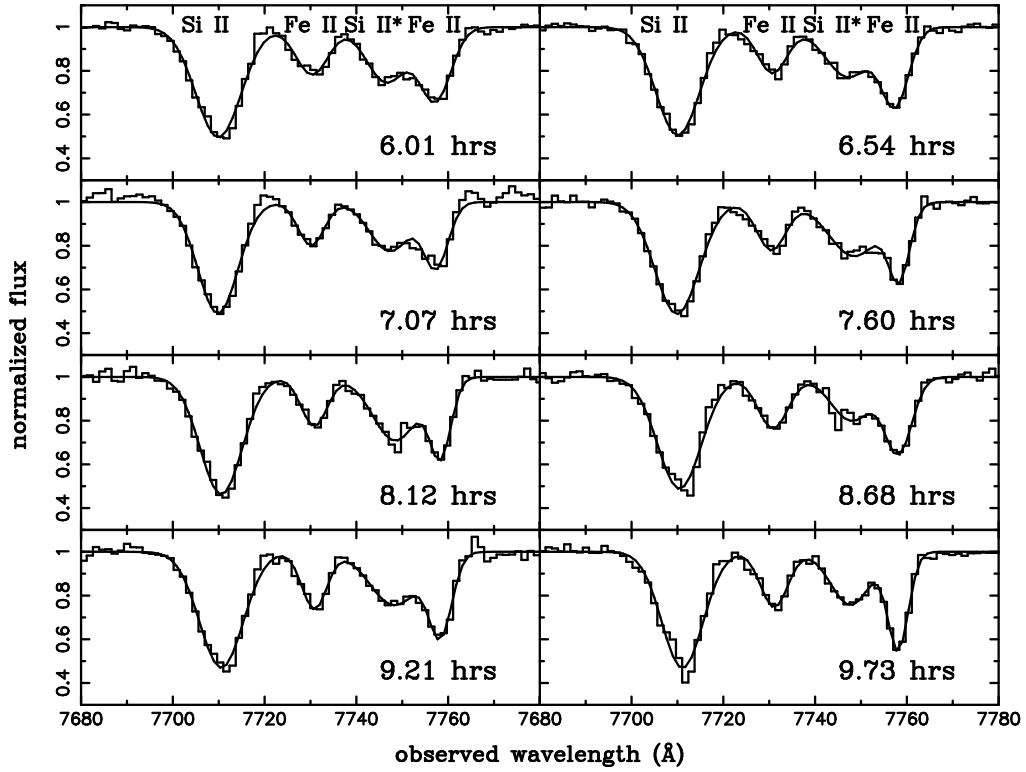
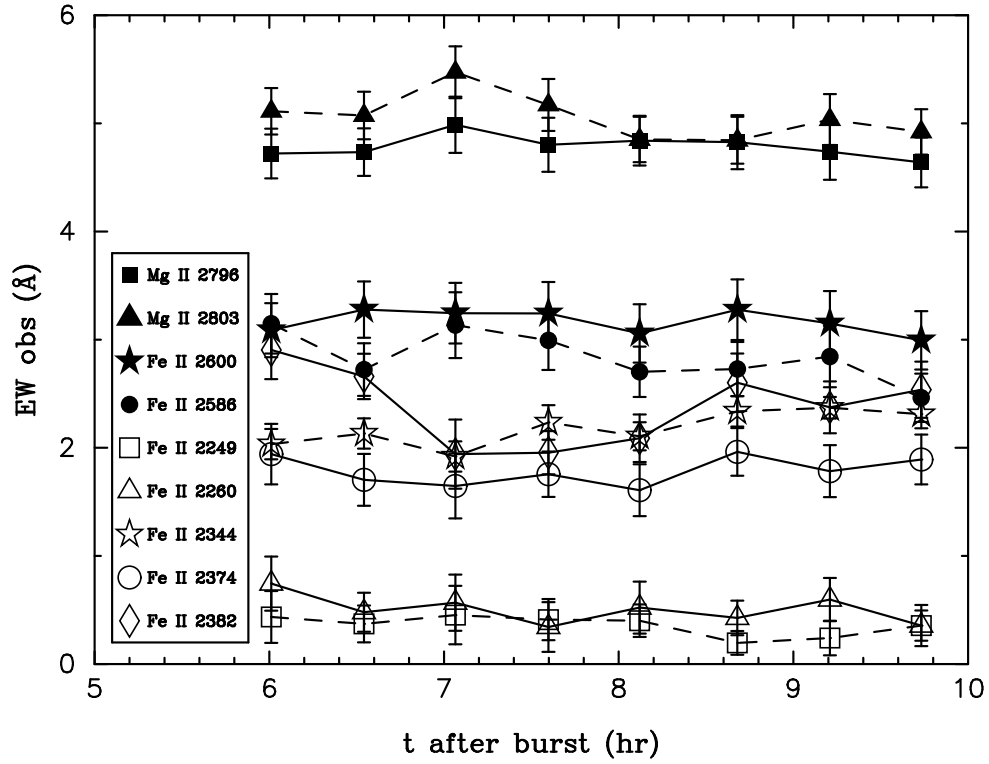


Fig. 8. The same as Fig. 2, but for Fe II  $\lambda$ 2344.2 at  $z = 2.26$ .





**Fig. 9.** The same as Fig. 2, but for Fe II  $\lambda\lambda 2374.5, 2382.8$  at  $z = 2.26$ . The absorption lines at  $7710 \text{ \AA}$  and  $7748 \text{ \AA}$  are Si II  $\lambda 1526.7$  and Si II\*  $\lambda 1533.4$  at  $z = 4.05$ , respectively.



**Fig. 10.** Equivalent widths (observer's frame) of the  $z = 2.26$  Mg II  $\lambda 2796.4$  (filled square), Mg II  $\lambda 2803.5$  (filled triangle), Fe II  $\lambda 2600.2$  (filled star), Fe II  $\lambda 2586.7$  (filled circle), Fe II  $\lambda 2249.9$  (open square), Fe II  $\lambda 2260.8$  (open triangle), Fe II  $\lambda 2344.2$  (open star), Fe II  $\lambda 2374.5$  (open circle), and Fe II  $\lambda 2382.8$  (open diamond) absorption lines, as functions of time after the burst.

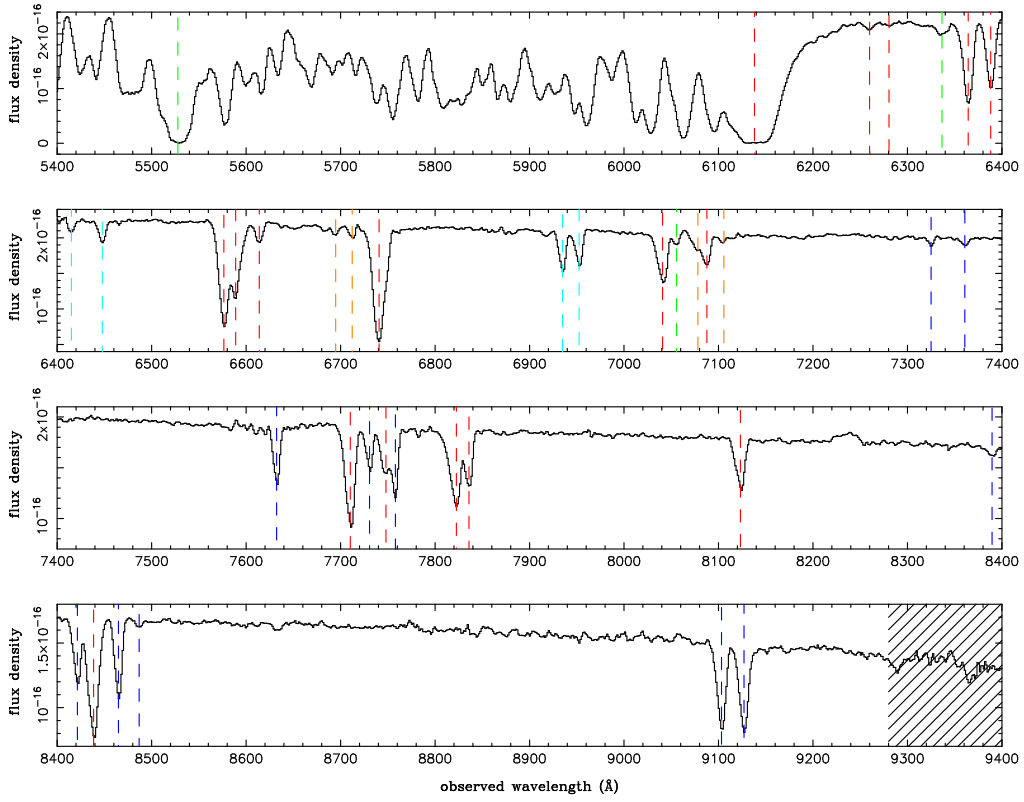


**Fig. 11.** The observed spectrum of GRB 060206 afterglow in vacuum wavelength. This high signal-to-noise ratio spectrum was made by combining all data. The hatched region between 9280 and 9600 Å indicates the place of water vapor absorption lines in the atmosphere. Red, green, blue and cyan dashed lines indicate absorption lines at  $z = 4.05, 3.55, 2.26$ , and  $1.48$ , respectively. The unidentified lines are indicated by orange dashed lines. See identifications in Table 3.

**Table 1.** Equivalent width (observer's frame) of the  $z = 1.48$  Absorption Lines.

Hour	$EW_{\text{FeII}2600}$	$EW_{\text{FeII}2586}$	$EW_{\text{MgII}2796}$	$EW_{\text{MgII}2803}$
6.011	$1.30 \pm 0.22$	$0.62 \pm 0.23$	$2.43 \pm 0.18$	$1.88 \pm 0.18$
6.542	$1.29 \pm 0.22$	$0.60 \pm 0.20$	$2.37 \pm 0.19$	$2.04 \pm 0.19$
7.065	$1.09 \pm 0.21$	$0.55 \pm 0.24$	$2.09 \pm 0.18$	$1.86 \pm 0.20$
7.598	$1.24 \pm 0.25$	$0.38 \pm 0.20$	$2.17 \pm 0.19$	$1.90 \pm 0.20$
8.120	$1.27 \pm 0.22$	$0.87 \pm 0.24$	$2.20 \pm 0.17$	$1.83 \pm 0.18$
8.679	$1.01 \pm 0.21$	$0.57 \pm 0.20$	$2.34 \pm 0.18$	$1.90 \pm 0.20$
9.209	$1.11 \pm 0.24$	$0.53 \pm 0.20$	$2.25 \pm 0.19$	$1.87 \pm 0.21$
9.732	$1.18 \pm 0.20$	$0.55 \pm 0.20$	$2.29 \pm 0.17$	$2.00 \pm 0.19$

**Table 2.** Equivalent width (observer's frame) of the  $z = 2.26$  Absorption Lines.

Hour	$EW_{\text{FeII}2600}$	$EW_{\text{FeII}2586}$	$EW_{\text{MgII}2796}$	$EW_{\text{MgII}2803}$
6.011	$3.09 \pm 0.25$	$3.15 \pm 0.28$	$4.72 \pm 0.23$	$5.11 \pm 0.22$
6.542	$3.28 \pm 0.26$	$2.72 \pm 0.24$	$4.73 \pm 0.22$	$5.07 \pm 0.22$
7.065	$3.24 \pm 0.28$	$3.13 \pm 0.30$	$4.99 \pm 0.26$	$5.47 \pm 0.24$
7.598	$3.24 \pm 0.29$	$2.99 \pm 0.27$	$4.80 \pm 0.25$	$5.17 \pm 0.24$
8.120	$3.06 \pm 0.27$	$2.70 \pm 0.23$	$4.84 \pm 0.23$	$4.85 \pm 0.21$
8.679	$3.28 \pm 0.28$	$2.73 \pm 0.25$	$4.83 \pm 0.25$	$4.84 \pm 0.22$
9.209	$3.15 \pm 0.30$	$2.84 \pm 0.28$	$4.74 \pm 0.26$	$5.04 \pm 0.24$
9.732	$2.99 \pm 0.27$	$2.46 \pm 0.22$	$4.64 \pm 0.23$	$4.92 \pm 0.21$

Hour	$EW_{\text{FeII}2249}$	$EW_{\text{FeII}2260}$	$EW_{\text{FeII}2344}$	$EW_{\text{FeII}2374}$	$EW_{\text{FeII}2382}$
6.011	$0.44 \pm 0.24$	$0.74 \pm 0.25$	$2.0 \pm 0.14$	$1.9 \pm 0.28$	$2.9 \pm 0.27$
6.542	$0.37 \pm 0.17$	$0.48 \pm 0.18$	$2.1 \pm 0.14$	$1.7 \pm 0.24$	$2.7 \pm 0.21$
7.065	$0.45 \pm 0.27$	$0.57 \pm 0.26$	$1.9 \pm 0.14$	$1.6 \pm 0.30$	$1.9 \pm 0.32$
7.598	$0.41 \pm 0.19$	$0.34 \pm 0.23$	$2.2 \pm 0.16$	$1.8 \pm 0.21$	$2.0 \pm 0.20$
8.120	$0.40 \pm 0.15$	$0.52 \pm 0.24$	$2.1 \pm 0.13$	$1.6 \pm 0.24$	$2.1 \pm 0.22$
8.679	$0.20 \pm 0.11$	$0.43 \pm 0.16$	$2.3 \pm 0.14$	$2.0 \pm 0.22$	$2.6 \pm 0.27$
9.209	$0.24 \pm 0.16$	$0.60 \pm 0.20$	$2.4 \pm 0.10$	$1.8 \pm 0.24$	$2.4 \pm 0.24$
9.732	$0.36 \pm 0.19$	$0.36 \pm 0.14$	$2.3 \pm 0.13$	$1.9 \pm 0.23$	$2.5 \pm 0.26$

**Table 3.** Line Identification

Wavelength ( $\text{\AA}$ )	Line	$z$	$W_r$ ( $\text{\AA}$ )	Ref.
5527.8	H I 1215.67	3.5471	–	1
6138.1	H I 1215.67	4.0492	–	2
6259.9	N V 1238.82	4.0531	$0.093 \pm 0.015$	3
6280.4	N V 1242.80	4.0534	$0.063 \pm 0.017$	3
6336.5	Si IV 1393.76	3.5463	$0.46 \pm 0.048$	1
6364.3	Si II 1260.42	4.0494	$1.6 \pm 0.017$	3
6388.1	Si II* 1264.74, 1265.00	4.0504	$1.1 \pm 0.016$	3
6415.1	Fe II 2586.65	1.4801	$0.20 \pm 0.027$	3
6447.8	Fe II 2600.17	1.4798	$0.48 \pm 0.033$	1, 3
6576.5	O I 1302.17	4.0504	$1.5 \pm 0.023$	3
6589.0	O I* 1304.86, 1306.03, Si II 1304.37	4.0487	$1.1 \pm 0.028$	3
6614.0	Si II* 1309.28	4.0516	$0.20 \pm 0.012$	3
6694.8	?	–	–	
6712.3	?	–	–	
6740.8	C II 1334.53, C II* 1335.66, 1335.71	4.0482	$2.2 \pm 0.019$	3
6935.0	Mg II 2796.35	1.4800	$0.93 \pm 0.031$	1, 3
6952.4	Mg II 2803.53	1.4799	$0.77 \pm 0.031$	1, 3
7040.8	Si IV 1393.76	4.0517	$0.79 \pm 0.017$	
7055.6	C IV 1550.77	3.5497	$0.092 \pm 0.011$	
7078.2	?	–	–	
7087.7	Si IV 1402.77	4.0527	$0.34 \pm 0.051$	
7105.7	?	–	–	
7325.0	Fe II 2249.88	2.2557	$0.10 \pm 0.0089$	
7360.7	Fe II 2260.78	2.2558	$0.14 \pm 0.012$	
7632.3	Fe II 2344.21	2.2558	$0.68 \pm 0.023$	
7710.3	Si II 1526.71	4.0503	$1.2 \pm 0.024$	
7730.6	Fe II 2374.46	2.2557	$0.55 \pm 0.029$	
7748.0	Si II* 1533.43	4.0527	$0.63 \pm 0.047$	
7758.0	Fe II 2382.77	2.2559	$0.74 \pm 0.061$	
7823.3	C IV 1548.20	4.0532	$0.69 \pm 0.15$	
7835.8	C IV 1550.77	4.0528	$0.51 \pm 0.016$	
8123.2	Fe II 1608.45	4.0503	$0.59 \pm 0.012$	
8389.5	Mn II 2576.88	2.2557	$0.17 \pm 0.024$	
8421.4	Fe II 2586.65	2.2557	$0.89 \pm 0.023$	

1: Hao et al. 2007, 2: Fynbo et al. 2006, 3: Thöne et al. 2008

**Table 3.** (Continued.)

Wavelength ( $\text{\AA}$ )	Line	$z$	$W_r$ ( $\text{\AA}$ )	Ref.
8438.6	Al II 1670.79	4.0507	$1.4 \pm 0.017$	
8464.9	Fe II 2600.17	2.2555	$0.98 \pm 0.020$	
8486.8	Mn II 2606.46	2.2561	$0.083 \pm 0.018$	
9103.2	Mg II 2796.35	2.2554	$1.5 \pm 0.029$	
9127.0	Mg II 2803.53	2.2555	$1.6 \pm 0.029$	